

# Methanol conversion on metal-incorporated SAPO-34s (MeAPSO-34s)

Misook Kang<sup>\*</sup>

*Department of Chemical Engineering, Dankook University, San 8, Hannam-dong, Youngsan-ku, Seoul 140-714, South Korea*

Received 28 February 2000; accepted 18 May 2000

## Abstract

The influence on metal incorporation into the framework of SAPO-34 (MeAPSO-34) on methanol conversion was investigated in this study. Used MeAPSO-34s (SAPO-34, FeAPSO-34, CoAPSO-34, and NiAPSO-34) were acquired by the rapid crystallization method. In characteristics, it was identified that these catalysts had a uniformly regular form with a sharp distribution in particle size. The performances on methanol conversion for these catalysts were different according to the properties of metals. As a result, the methanol conversion was enhanced on the metal-incorporated catalyst compared with the non-metal catalyst. In reaction at 450°C for 1 h, the order of increasing in ethylene selectivity was followed as next; Ni- > Co- > Fe- > non-metal-incorporated SAPO-34. On the other hand, the selectivity for all the samples decreased with an increase in reaction time, however, the reduced rate was very slow on CoAPSO-34 compared with the other catalysts. In addition as a surprising result, the CoAPSO-34 catalyst exhibited a minor methanation. © 2000 Elsevier Science B.V. All rights reserved.

**Keywords:** Rapid crystallization method; MeAPSO-34s; Methanol conversion; Ethylene selectivity; Methanation

## 1. Introduction

The synthesis of light olefins in petroleum chemistry have been more interesting and important recently. These valuable intermediate compounds, light olefins, are easily hydrogenated into chemically stable and undesired light paraffins. Therefore, to obtain target product, the controls of many factors, for example like its acidity, pore size, and distribution of

particle size, which had close influence on catalytic performance, must be necessary.

On the other hand, after the innovation in the synthesis of aluminophosphate molecular sieves by UCC [1], a trial for light olefin synthesis from methanol had been done using SAPO-34 as the catalyst [2–5]. A rather high selectivity to ethylene and propylene was observed without causing serious coke formation, although the catalyst has an isomorph of chabazite. Remarkable results were then found by using NiAPSO-34 [6–8], on which ethylene was obtained as a selectivity of 88% with 100% methanol conversion without coke formation.

However, it was suggested in our previous papers [7,8] that the extra-framework nickel

<sup>\*</sup> Present address: Department of Chemical Engineering, Sungkyunkwan University, Chonchondong 300, Janganku, Suwon 440-946, Korea. Tel.: +82-31-290-7275; fax: +82-31-290-7272.

E-mail address: msk1205@chollian.dacom.co.kr (M. Kang).

component relates closely to the methanation activity which resulted in decreased of ethylene selectivity in methanol conversion. In order to restrain the adverse effect of extra-framework nickel ingredient, the influence on sulfidation by  $\text{SO}_2$  or  $\text{H}_2\text{S}$  addition in methanol conversion was investigated. Subsequently, it was established that these sulfidation treatments could control the methane yield on methanol conversion; with addition of  $\text{H}_2\text{S}$ , methane yield decreased to a half of selectivity compared with the reaction without addition of  $\text{H}_2\text{S}$ . However, these sulfur compounds are a concerning problem for air pollution. Therefore, in this present study, it was tried to synthesize CoAPSO-34 crystal substituting cobalt for nickel, and it was applied to the methanol conversion reaction expecting to decrease the methanation.

Furthermore, the characterization of cobalt species in cobalt-containing molecular sieves has been the subject of many investigations [9–13]. In particular, most of these reports had deal with the substitution of Al by bivalent metal ions, creating Brönsted acid sites, namely acidic P–OH groups, as well as Lewis acid sites. Consequently, reduction of  $\text{Me}^{3+}$  to  $\text{Me}^{2+}$  in MeAPOs leads to the increase in the concentration of acidic sites.

However, the real nature and properties of these acidic sites in MeAPOs and isomorph of MeAPSOs have still remained unclear, and the reports for the hydrocarbon synthesis using MeAPSO-34 are very scarce.

Therefore, in this work, synthesis and characterization for SAPO-34s, which contained transition metals of high concentration, were investigated. In particular, their performances on methanol conversion were observed in detail.

## 2. Experimental

### 2.1. Preparation of catalyst

Metal-containing SAPO-34s (MeAPSO) were synthesized using the concept of the rapid crys-

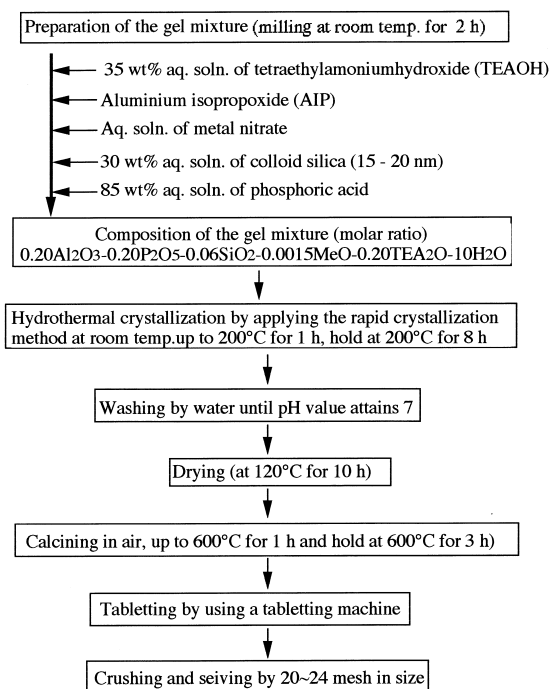


Fig. 1. Preparation procedure of the metal-incorporated SAPO-34 catalysts.

tallization method [14]. In Fig. 1, the typical preparation procedure of these catalysts is shown. Used reagents for the preparation of gel mixture were as follows: 35 wt.% aqueous solution of tetraethyl ammonium hydroxide (TEAOH, Aldrich) was used as the organic template. Aluminum isopropoxide (AIP, Wako), cataloid-30 (30 wt.%  $\text{SiO}_2$ , Kasei Tesque), and phosphoric acid (85 wt.%  $\text{H}_3\text{PO}_4$ , Nacali Tesque) were used as the starting materials of Al, Si, and P ingredients, respectively. Nitrate hydrate forms from Nacalai Tesque were used as metal sources.

### 2.2. Characterization

The crystallinity and phase purity of the samples synthesized here were identified by powder X-ray diffraction (XRD) using Shimadzu XD-DI

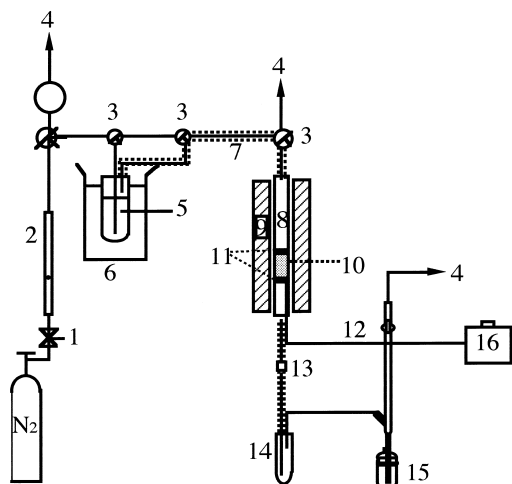


Fig. 2. Schematic diagram of fixed-bed flow-type reaction apparatus. (1) Needle valve; (2) flow meter; (3) three-way stop-cock; (4) purge; (5) MeOH; (6) water bath; (7) ribbon heater; (8) tubular reactor; (9) electric furnace; (10) catalyst; (11) quartz wool; (12) thermocouple; (13) sampling port; (14) trap; (15) soap-film flow meter; (16) temperature controller.

with Nickel filtered Cu  $K\alpha$  radiation (30 kV, 30 mA) in the  $2\theta$  range from  $5^\circ$  to  $50^\circ$ .

Chemical compositions in crystal were analyzed by inductively coupled plasma (ICP), Shimadzu ICPS-1000III.

Crystal size and shape of catalysts were observed by using Hitachi S-2500CX scanning electron microscope (SEM).

BET surface areas of crystals were measured by nitrogen gas adsorption at the liquid nitrogen temperature in mixed gas of nitrogen and helium flow as the carrier gas with Shimadzu Flow sorbs 2–2300.

Particle size distribution was measured by diffraction of light scattering (DLS) system of Photol Otsuka Electronics; the samples were dispersed by an ultrasonic wave treatment for 10 min with 120 W in water. The analysis was determined by weight based distribution.

The acidity of catalyst was estimated by TPD profiles of pre-adsorbed  $\text{NH}_3$ , determined by Quadruple Mass Spectrometer [(M-QA100F) of BEL JAPAN]. To restrain the influence of water during  $\text{NH}_3$  adsorption, the adsorption was done at higher temperatures than  $100^\circ\text{C}$ .

### 2.3. Catalytic reaction

Each methanol conversion reaction was carried out using an ordinary continuous flow reactor as shown in Fig. 2. A 0.325-g portion (0.35 ml) of the catalyst was packed into a quartz tubular reactor having 0.5 cm inner diameter, and a reaction gas, which was composed of 15 mol% methanol and 85 mol%  $\text{N}_2$ , was allowed to flow with a gaseous space velocity (GHSV) of  $1000\text{ h}^{-1}$  at  $450^\circ\text{C}$  for 1 h.

The products were analyzed by three FID-type gas chromatographs, Shimadzu GC7A, 12A, and 14A, equipped with integrators. Analyses for methanol and dimethyl ether,  $\text{C}_1$ – $\text{C}_4$  hydrocarbons, and gasoline range hydrocarbons were carried out by using columns porapark T, VZ-10, and silicon OV-101, respectively.

The amount of coke deposited on the catalyst after the reaction was measured by temperature-programmed oxidation (TPO) on a Shimadzu DT-40 thermo-gravimeter with a heating rate of  $10^\circ\text{C}/\text{min}$  in a 40 ml/min air flow. The profiles were calculated from the weight-loss from  $300^\circ\text{C}$  to  $800^\circ\text{C}$ .

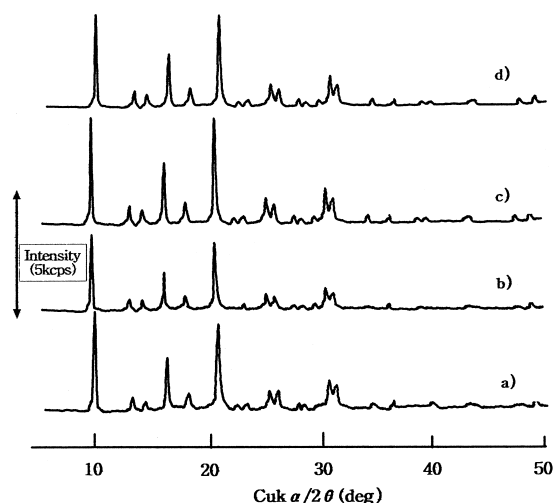


Fig. 3. XRD pattern for as-synthesized crystals; (a) SAPO-34, (b) FeAPSO-34, (c) CoAPSO-34, and (d) NiAPSO-34.

### 3. Results and discussion

#### 3.1. Characteristics of metal-incorporated SAPO-34s

In Fig. 3, the XRD patterns of attained crystals are shown. These patterns were the same to that of CHA type silicoaluminophosphate in the US patent [2]. Judging from the XRD, it can be said that the MeAPSO-34 was successfully synthesized. Especially, the CoAPSO-34 crystal was a strong intensity in XRD pattern compared with the other metal-incorporated crystals.

Morphology of the crystals, which observed by SEM photograph, is shown in Fig. 4. As shown in this figure, all the samples had uniform cubic crystals with chabazite-like structure. The catalyst with the nickel component was smaller than the other catalysts. On the other hand, the particle size distribution was broader in FeAPSO-34 than the other catalysts. This result shows that the crystallization rates for all the catalysts were different according to incorporated metal species without consistency.

These results are also accorded to Fig. 5. The particle sizes decreased in catalysts with Ni or

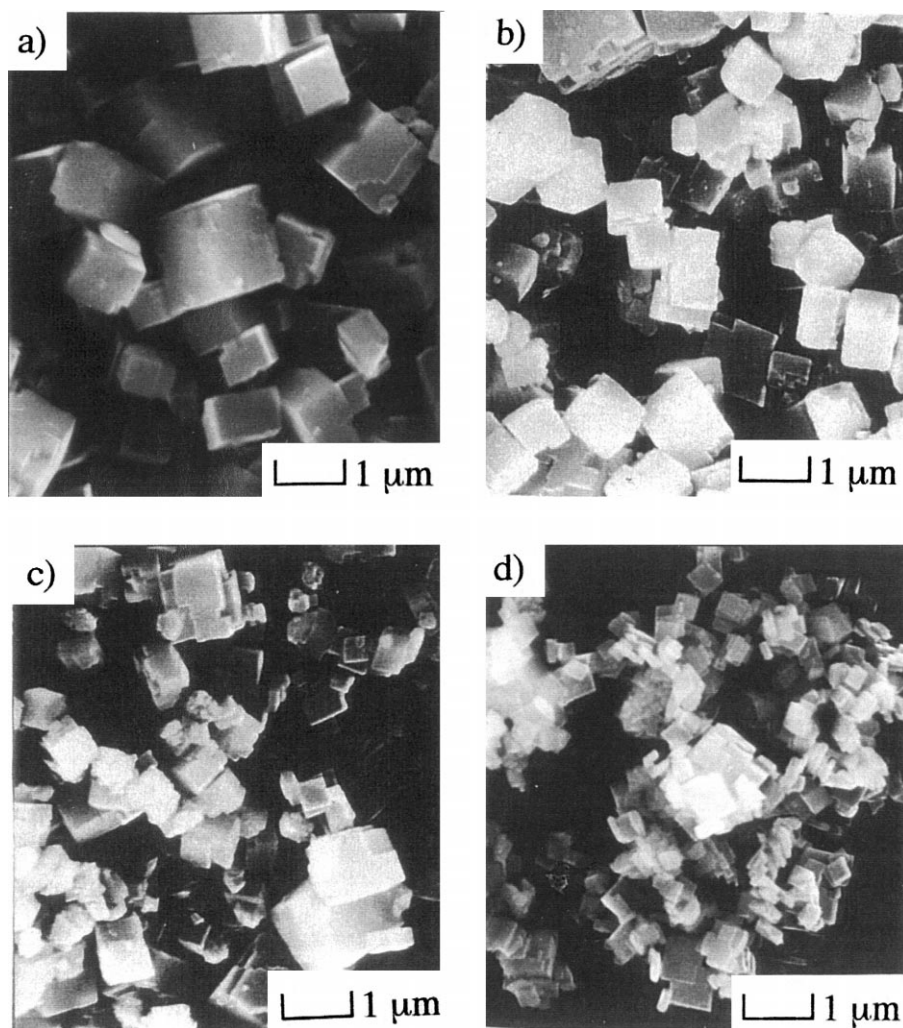


Fig. 4. SEM photographs of MeAPSO-34 crystals. (a) SAPO-34, (b) CoAPSO-34, (c) FeAPSO-34, and (d) NiAPSO-34.

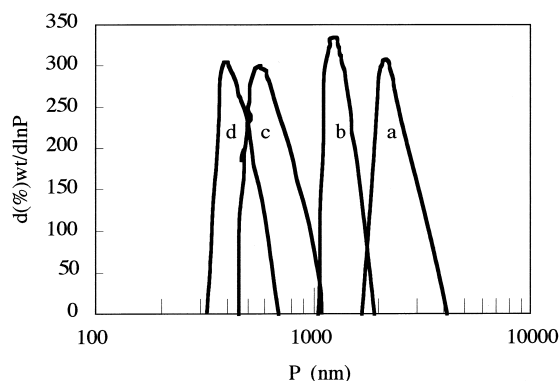


Fig. 5. Distribution of particle size for MeAPSO-34 crystals. (a) Si/Me =  $\infty$ :2117\*, (b) Si/Co = 40:1505\*, (c) Si/Fe = 40:950\*, and (d) Si/Ni = 40:800\*, \* average particle size (nm).

Fe component, however, the distribution in particle size was shown as a sharp style in CoAPSO-34.

Table 1 depicts compositions in synthesized crystals, which were analyzed by ICP test. As shown, the Co amount in crystal was higher than the other metals in spite of the same amount in gel mixtures. This result relatively shows that incorporation of Ni or Fe into framework was very difficult, and much metals which remained out of the framework were identified from UV–visible spectra test [7]. On the other hand, the BET surface areas possessed wide areas above 490 m<sup>2</sup>/g for all the catalysts.

### 3.2. Acidic property

The NH<sub>3</sub>–TPD profiles are shown in Fig. 6. Zeolitic materials possess lots of acid sites and certain acidic strengths attributed to their high

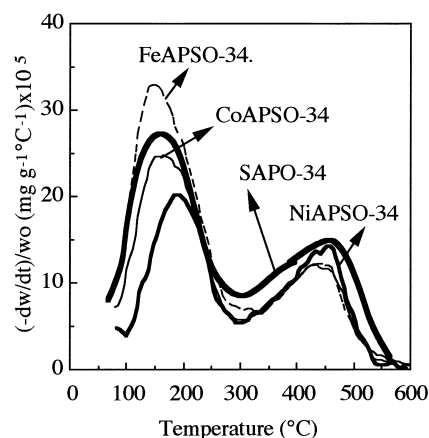


Fig. 6. NH<sub>3</sub>–TPD profiles of metal-incorporated SAPO-34 catalysts.

Al contents and tetrahedral Al sites, respectively. In general, aluminophosphates (AlPO<sub>4</sub>-n) are prepared in the presence of cation or neutral amine additives and crystallize with a composition ratio of Al/P of one, resulting in no net charge on the framework. However, as the addition of silica (SAPO) and/or other metal ions to the structure, it was introduced changes in both of catalytic capacity and acidity. In particular, the incorporation of silica into framework displayed Brønsted acid sites. Therefore, if the Si is substituted by other transition metals, the acid sites should be decreased. On the other hand, these profiles consist of two peaks: one appears at a low temperature range 130–220°C and another appears at a high temperature range 400–500°C. These low and high desorption peaks correspond to the weak and strong acid sites, respectively. As shown in Fig. 6, all

Table 1  
Physical properties of MeAPSO-34 catalysts

| Catalysts           | Composition in crystals<br>(atomic ratio) |      |      |        | Surface area<br>(m <sup>2</sup> /g) | Size of particle<br>(μm) |
|---------------------|---|------|------|--------|-------------------------------------|--------------------------|
|                     | Al  | Si   | P    | Me     |                                     |                          |
| SAPO-34             | 1.00                                      | 0.30 | 0.69 | –      | 502                                 | 1.5–2.0                  |
| FeAPSO-34           | 1.00                                      | 0.27 | 0.69 | 0.0038 | 486                                 | 0.8–1.5                  |
| CoAPSO-34           | 1.00                                      | 0.32 | 0.65 | 0.0078 | 525                                 | 1.2–15                   |
| NiAPSO-34           | 1.00                                      | 0.29 | 0.73 | 0.0029 | 498                                 | 0.8–1.0                  |
| Experimental method | ICP                                       |      |      |        | BET                                 | SEM                      |

MeAPSO-34 catalysts exhibited lower acidity and acid sites compared with the non-metal catalyst. In particular, in case of the NiAPSO-34, the acidity at high temperature increased compared with that on the other catalysts. However, at low temperature, the acid sites increased as follows: Fe- < Co- < Ni-incorporated materials. In general, the acid site was important as well as the strength, in particular, all the acid sites have been considered in ethylene synthesis from methanol.

### 3.3. Catalytic performance

In Fig. 7, methanol conversion and selectivity to ethylene for MeAPSO-34 catalysts at various reaction temperatures are shown. As shown, the methanol conversions for all the catalysts were almost the same as 95% at all reaction temperatures. On the other hand, the selectivity to ethylene increased on metal-incorporated catalysts compared with non-metal catalyst. At 450°C, the order in ethylene selectivity was followed as next; NiAPSO-34 > CoAPSO-34 > FeAPSO-34 > non-metal SAPO-34. In particular, the selec-

tivity to ethylene was the highest as above 70% in NiAPSO-34.

Fig. 8 shows product distribution on methanol conversion at 425°C after 1 h. The methanol conversion exhibited above 90% for all the catalysts. On the other hand, the product distributions were various. As shown, the ethylene selectivity was the highest in NiAPSO-34 as above 80%, and then the order in ethylene selectivity was followed as next; SAPO-34 < CoAPSO-34 < FeAPSO-34 < NiAPSO-34. This result is related that a small particle size and a little acid site in catalysts enhanced the ethylene selectivity on methanol conversion. As a surprising result, the methane selectivity remarkably decreased in CoAPSO-34 compared with the other catalysts which exhibited about 10% methane selectivity. Therefore, it was confirmed that introduction of Co in place of Ni was useful for the decrease of methanation.

Results of the duration test are shown in Fig. 9. As shown, the conversion of methanol and selectivity to ethylene decreased for all the catalysts with an increase in time on stream. However, the decreasing tendencies were various.

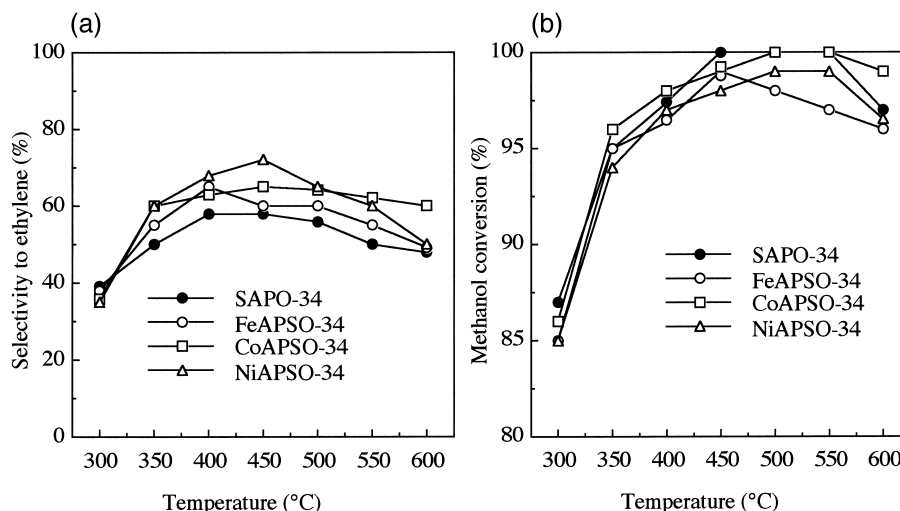


Fig. 7. Effect of reaction temperature on methanol conversion for MeAPSO-34 catalysts. (a) Selectivity to ethylene and (b) methanol conversion; reaction condition; time 1 h, 20–24 mesh, GHSV: 1000 h<sup>-1</sup>; Gas condition; MeOH 15 mol%–N<sub>2</sub> 85 mol%.

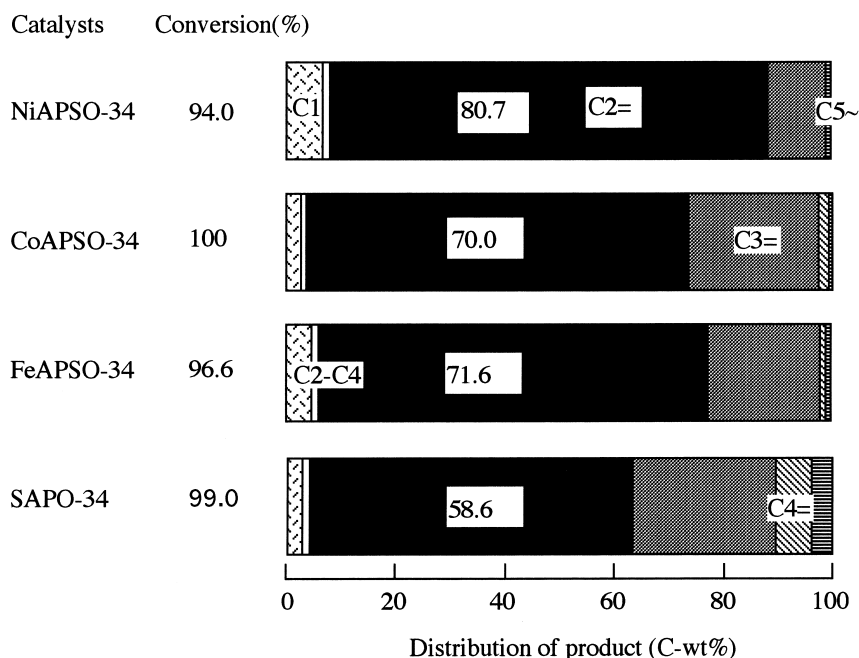


Fig. 8. Distribution of product on methanol conversion reaction for MeAPSO-34 catalysts. Reaction conditions; time 1 h; GHSV:  $1000 \text{ h}^{-1}$ ; temperature:  $425^\circ\text{C}$ . Gas condition; MeOH 15 mol%– $\text{N}_2$  85 mol%.

The 100% conversion in SAPO-34 and CoAPSO-34 were maintained for 5 h and then it decreased abruptly until 85%. However, in cases of NiAPSO-34 and FeAPSO-34, the methanol conversion decreased slowly until 85% conver-

sion after 4 h. On the other hand, the ethylene selectivities on NiAPSO-34 and CoAPSO-34 decreased slowly with an increase of time on stream, while the selectivities decreased abruptly until 40% on SAPO-34 and FeAPSO-34.

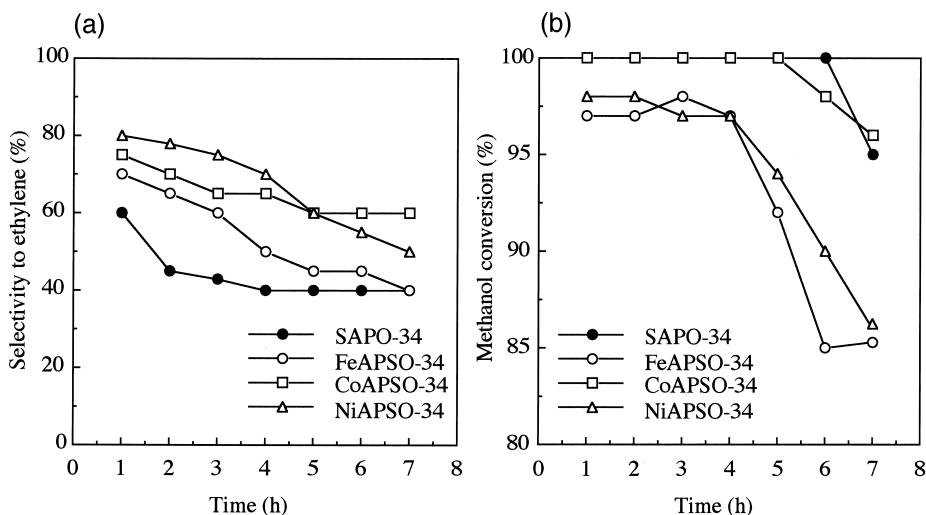


Fig. 9. Effect of time on stream on selectivity to ethylene and methanol conversion. (a) Selectivity to ethylene and (b) methanol conversion; reaction condition; temperature:  $425^\circ\text{C}$ ; GHSV  $1000 \text{ h}^{-1}$ . Gas composition; MeOH 15 mol%– $\text{N}_2$  85 mol%.

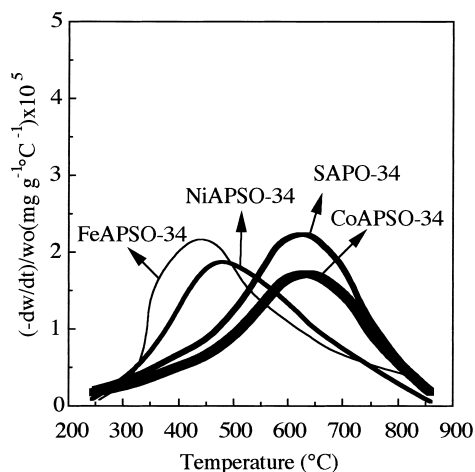


Fig. 10. Deposited coke amount on MeAPSO-34 after reaction. Reaction condition; temperature: 425°C; time 5 h, 20–24 mesh, GHSV 1000 h<sup>-1</sup>. Gas composition; MeOH 15 mol%–N<sub>2</sub> 85 mol%.

After the reaction, the coke deposited on the catalysts was analyzed by TPO and the profiles are shown in Fig. 10. For SAPO-34 and CoAPSO-34, the amount of deposited coke increased and the coke combustion temperature shifted to high temperatures. On the other hand, compared with pure SAPO-34, the coke combustion temperature was lower on FeAPSO-34 and NiAPSO-34. This is ascribing to the decreased in the number of acid sites and particle size on FeAPSO-34 and NiAPSO-34 compared with the other catalysts.

#### 4. Conclusions

This study had been focused on the influence of transition metals incorporation into framework of SAPO-34 on methanol conversion. The results could be summarized as follows.

(1) By rapid crystallization method, the metal-incorporated crystals having a high crystallinity and a sharp distribution in particle size were obtained.

(2) The performances for methanol conversion on these catalysts were exhibited variously;

the methanol conversion on the metal-incorporated materials was enhanced compared with the non-metal material.

(3) The Ni-incorporated SAPO-34 exhibited the highest ethylene selectivity on methanol conversion compared with the other catalysts.

(4) The CoAPSO-34 catalyst exhibited a minor methanation in methanol conversion compared with the other catalysts.

(5) The ethylene selectivity and methanol conversion decreased for all the catalysts with an increase in time on stream, however the conversion of 60% and methanol conversion of 98% in CoAPSO-34 were kept until 6 h. This result is ascribed to decrease in methane selectivity which resulted in catalytic deactivation.

(6) For SAPO-34 and CoAPSO-34, the amount of deposited coke increased and the coke combustion temperature shifted to high temperatures, however the combustion temperature was low on FeAPSO-34 and NiAPSO-34. This result is ascribed to the strength of acidity.

#### References

- [1] J. Haggin, Chem. Eng. News 20 (1983) 36, June.
- [2] S.T. Wilson, B.M. Lok, and E.M. Flanigen, US patent 4310440 (1982).
- [3] T. Inui, H. Matsuda, H. Okaniwa, A. Miyamoto, Appl. Catal., A: General 58 (1990) 155.
- [4] J. Liang, H. Li, S. Zhao, W. Guo, R. Wang, M. Ling, Appl. Catal., A: General 64 (1990) 31.
- [5] J.M. Thomas, Y. Xu, C.R.A. Catkow, J.W. Coaves, Chem. Mater. 3 (1991) 667.
- [6] T. Inui, S. Phatanasri, H. Matsuda, J. Chem. Soc., Chem. Commun. (1990) 205.
- [7] M. Kang, T. Inui, Catal. Lett. 53 (1999) 171.
- [8] T. Inui, M. Kang, Appl. Catal., A: General 164 (1997) 211.
- [9] M.G. Uytterhoeven, R.A. Schoonheydt, Micro. Mater. 3 (1994) 265.
- [10] J.A. Martens, M. Mertens, P.J. Grobet, P.A. Jacobs, Stud. Surf. Sci. Catal. 37 (1988) 97.
- [11] S.T. Wilson, Stud. Surf. Sci. Catal. 58 (1991) 137.
- [12] H.-S. Han, H. Chon, Micro. Mater. 3 (1994) 331.
- [13] L.E. Iton, I. Choi, J.A. Desjardins, V.A. Maroni, Zeolites 9 (1989) 535.
- [14] M. Kang, M.-H. Um, T. Inui, J. Mol. Catal. A: Chem. 150 (1) (1999) 195.